

Amira Aboussalih,
Salah Hammoudi,
Kamel Fedaoui,
Karim Arar,
Lazhar Baroura

EVALUATION OF PRAGER AND CHABOCHE MODELS FOR RELIABLE PREDICTION OF ELASTOPLASTIC BEHAVIOUR IN LOW-CYCLE FATIGUE

The object of this research is the cyclic elastoplastic behavior of materials, principally austenitic stainless steel (304L). The paper studies the 304L stainless steel behavior of exposed to different uniaxial and multiaxial cyclic loadings. It also determines the accuracy with which classical models, such as the Prager model, reproduce the phenomena of work hardening. All the models have which limits the reliability of fatigue life predictions for structures. For that, in this numerical study, a comparative analysis is performed between the Prager model and the Chaboche model. Chaboche model was selected to overcome the shortcomings of classical approaches, it can incorporate isotropic and nonlinear kinematic work hardening together. Numerous numerical simulations were conducted under various loading scenarios allowed to estimate the predictive capacity of the constitutive models and the limitations of simplified linear approaches. The results obtained, show that Chaboche model reproduces with excellent accuracy the phenomena of work hardening, additional work hardening, and ratcheting compared to the Prager model. This is explained by the fact that the Chaboche model can take into account the coupling between different phenomena which guarantees a realistic representation of cyclic elastoplastic behavior. Compared to similar models known in the literature, the Chaboche approach offers significant advantages: increased predictive accuracy, better representation of complex cyclic phenomena, and a fatigue life assessment of 304L stainless steel that closely reflects reality in demanding industrial applications.

Keywords: Prager model, Chaboche model, 304L SS, cyclic, ratcheting, hardening, fatigue.

Received: 16.09.2025

Received in revised form: 20.11.2025

Accepted: 12.12.2025

Published: 29.12.2025

© The Author(s) 2025

This is an open access article
under the Creative Commons CC BY license
<https://creativecommons.org/licenses/by/4.0/>

How to cite

Aboussalih, A., Hammoudi, S., Fedaoui, K., Arar, K., Baroura, L. (2025). Evaluation of Prager and Chaboche models for reliable prediction of elastoplastic behaviour in low-cycle fatigue. *Technology Audit and Production Reserves*, 6 (1 (86)), 34–42. <https://doi.org/10.15587/2706-5448.2025.339423>

1. Introduction

Modelling the behavior of elastoplastic materials used in much industrial installation is very important task to estimate their lifetime, principally when this element is subject to cyclic loading that can causes fatigue phenomena and to crack propagation [1]. These phenomena observed have a big responsibility in failures of structural and industrial systems [2].

A great method was developed in [3] that permit the prediction of the deformation over time, as well as the increase of damage resulting to failure, which is indispensable for continuing solicitations. In paper [4], mechanical structures made from in metallic materials and exposed to cyclic loading reveal very complex behaviors, like isotropic and kinematic hardening, stress relaxation, and cyclic softening. These mechanisms affect directly the development of stresses and strains over time.

While classical plasticity models proposed are based on the von Mises criterion, isotropic and kinematic hardening, and Prager model and Armstrong-Frederick laws, they stay incomplete and restricted in the representation of complex cyclic loading phenomena, such as ratcheting, saturation, or memory effects [5].

All these phenomena were represented by various constitutive models inspired by authors from plasticity theory. Between the classical approaches, Prager law simple and easy to implement, stays restricted in its capacity to define certain phenomena such as the ratchet effect [6, 7].

To overcome these limitations, Chaboche model occupies a prominent place. It introduces two mechanisms simultaneously: the expansion of the plasticity surface and the translation of its center in stress space, while adopting the von Mises plasticity criterion [8]. The use of these two effects corresponding respectively to isotropic hardening and nonlinear kinematic hardening permits a more realistic reproduction of the cyclic behavior of materials [9].

Chaboche model was extended to new version by taking into account the temperature and strain dependence [10]. Explicit and implicit integration schemes was compared and applied to the Chaboche isotropic-kinematic model, it have revealed that the explicit method, very faster, becomes unstable for large time steps, while the implicit approach gives good precision and stability, at the cost of superior computational effort [11].

These robust models are widely implemented in large FEA software, where they are essential tools for evaluating the fatigue life of components exposed to severe thermomechanical loading conditions [12].

The complex multiaxial elastoplastic cyclic behavior of structures made from steels has also been the subject of numerous studies, highlighting the need to refine multiaxial constitutive models to better prediction of the actual answers of materials, mostly in functional applications [13].

Although the wide diversity of proposed material constitutive models, rigorous computational a validation remains important to evaluation of their abilities. Simulation studies must be conducted to evaluate

the model responses under diverse loading situations and compare the predicted stress-strain curves with experimental data. These comparisons between models allow to define the accuracy of each of them and to identify its limitations to reproduce phenomena such as cyclic softening, or mean stress relaxation. Furthermore, the computational performance of the integration algorithms in terms of stability, convergence, and time efficiency must be analyzed to guarantee their fitness for large-scale numerical simulations. This phase is critical for bridging the gap between the formulation of the theoretical model and its reliable engineering application.

Researchers and engineers for a long time study 304L stainless steel because it is one of the most widely used stainless-steel grades, and understanding its behavior is essential for improving performance in real-world applications. Studying its behavior under cyclic loading helps ensure safety, durability, and reliability in a lot of industries such as chemical processing, food production, construction, and medical equipment. This new investigation helps to better material choice and a development of more resistance and long-life components.

Therefore, *the object of this research* is the cyclic elastoplastic behavior of materials, principally austenitic stainless steel (304L). This take in consideration the research and comparison of constitutive models in order to identify the best model for predicting the material's response under cyclic loading.

The aim of this research is the evaluation of Prager and Chaboche models for predicting the behavior of elastoplastic material under low-cycle fatigue. To achieve the set aim, the *following tasks* must be completed:

1. To achieve numerical computation on 304L stainless steel under cyclic loading.
2. To study and analyze the capacity of each model to represent uniaxial hardening, over-hardening, and ratcheting phenomena in material.
3. To estimate what is the isotropic and nonlinear kinematic hardening effects on cyclic material behavior.
4. To determine the best model for reliable finite element computation of material subject to cyclic elastoplastic behavior.

2. Materials and Methods

2.1. Materials

This section presents the constitutive model describing the material's elastoplastic behavior, where total axial strain is the sum of elastic and plastic components. The von Mises criterion defines the elastic limit and the onset of plastic flow. The material used in this study is a 304L SS, an austenitic chromium-nickel stainless and heat resistant steel with high toughness even at cryogenic temperatures due to its austenitic structure. It is used for many applications like automotive, machinery and nuclear engineering. All this for its great combination of strength, ductility and corrosion resistance. The chemical composition, see Table 1 and the mechanical properties can be found in [10].

Table 1
Chemical composition of 304L (%)

C	Si	Mn	P	S	Cr	Ni	Nb	Co	N
0.04	0.52	1.09	0.019	0.014	17.5	9.3	0.57	0.028	0.33

The axial strain is composed of two components expressing two different mechanisms

$$\varepsilon^T = \varepsilon^e + \varepsilon^p, \quad (1)$$

where ε^T – the total strain tensor; ε^e – the elastic strain tensor; ε^p – the plastic strain tensor. The elastic domain is given by von Mises yield criteria given in equation

$$f \nparallel J(\underline{\sigma} - \underline{R}) - \sigma_{yi}, \quad (2)$$

where f – the yield function; J – the second invariant of the tensor deviator of stress.

2.2. Prager law

Prager law describes the elastoplastic behavior of a material with a flow surface represented by a linear kinematic variable \underline{X} . It assumes that the movement of the yield surface center is proportional to the plastic strain.

The linear kinematic hardening law [3] is written

$$\underline{X} = C \varepsilon^p, \quad (3)$$

where \underline{X} – kinematic backstress variable; C – hardening modulus constant; ε^p – plastic strain.

2.3. Chaboche law

The elastoplastic model of Chaboche simulates the response of material when it is put into service by the combination of the two hardenings, isotropic R and kinematic nonlinear \underline{X} .

Isotropic Hardening: The evolution of the isotropic hardening is governed by the following equation

$$dR = b(Q - R)dp, \quad (4)$$

where Q and b – two material parameters; Q – the maximum value of R while b controls the kinetics.

The Non-linear Kinematic Hardening: This can be written in its simplest form as

$$d\underline{X} = \frac{2}{3} C(p) d\underline{\varepsilon}^p - \gamma(p) \underline{X} dp, \quad (5)$$

where C and γ – some material parameters; $d\underline{\varepsilon}^p$ – plastic strain and p – the accumulated plastic strain which may be deduced from

$$dp = \left[\frac{2}{3} d\underline{\varepsilon}^p : d\underline{\varepsilon}^p \right]^{1/2}. \quad (6)$$

The evolution of the kinematic variable was proposed through the superposition of m variables [14]

$$\underline{X} = \sum_1^m X_i, \quad (7)$$

$$\dot{\underline{X}}_m = \frac{2}{3} C_m \dot{\underline{\varepsilon}}^p - D_m X_m \left\langle 1 - \frac{X_1}{J(X_m)} \right\rangle p, \quad (8)$$

where C_m and D_m – some material parameters which may depend on the accumulated plastic strain p ; $J(X_m)$ – the von Mises equivalent stress of the tensor X_m ; $\langle \rangle$ – the MacCauley bracket, $\langle X \rangle = 0$ if $X \leq 0$ and $\langle X \rangle = X$ if $X > 0$.

2.4. Comparison between Prager law and Chaboche model

Table 2 presents the key aspects of Prager and Chaboche models, showing how Chaboche formulation advances beyond Prager law and its relevance in reproducing certain plasticity phenomena.

Fig. 1 illustrates the difference between linear and nonlinear kinematic hardening in the principal stress space (2D).

Table 2
Comparison between Prager law and Chaboche model

Aspect	Prager law	Chaboche model
Type of hardening	Linear kinematic hardening	Non-linear kinematic hardening
Mathematical form	$X = C\varepsilon^p$ (single linear term)	<ul style="list-style-type: none"> – Isotropic hardening $dR = b(Q - R)dp$. – The non-linear kinematic hardening $d\underline{X} = \frac{2}{3}C(p)d\varepsilon^p - \gamma(p)\underline{X}dp$
Number of parameters	Few (simple formulation)	Several parameters (greater flexibility)
Phenomena captured	Basic Bauschinger effect	Bauschinger effect, cyclic hardening/softening, ratcheting
Complexity	Simple and easy to implement	More complex, suitable for realistic cyclic loading
Limitations	Cannot model ratcheting or saturation	Can account for load history, ratcheting, and shakedown
Displacement of the yield surface (Fig. 1)	Linear: Along a straight path, without any change in shape or saturation	Nonlinear: Nonlinear, with a term that introduces progressive saturation

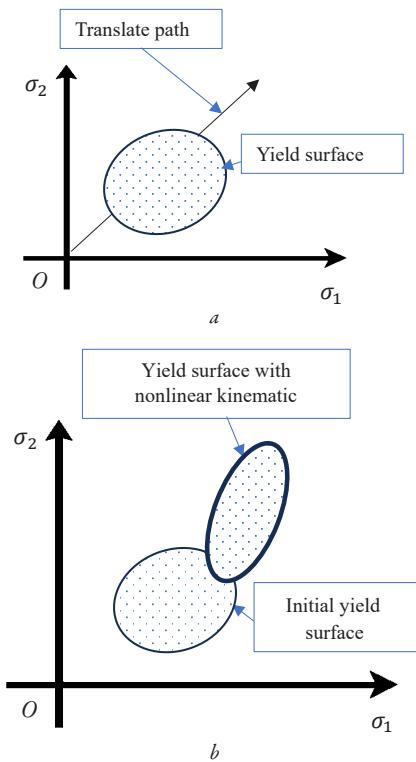


Fig. 1. Difference between linear and nonlinear kinematic hardening in the principal stress space (2D): *a* – linear kinematic; *b* – nonlinear kinematic

Fig. 1, *a* shows a simple translation characterized by a constant shape without saturation, whereas Fig. 1, *b* depicts a translation associated with a change in shape, reflecting nonlinear effects and the complex phenomena of cyclic behavior.

3. Results and Discussion

3.1. Validation of the material parameters

For the validation of numerical results from numerical computation with the experimental data must be down to guarantee the reliability of the chosen model before carrying out further simulations. Fig. 2 presents the superposition of cyclic hysteresis curves obtained from simulation and experiment down on 304L stainless steel under an imposed plastic strain of 0.5%.

The ZeBuLon finite element code was used in all the computation. simulated curve generated using the ZeBuLon, based on material parameters reported in the literature, whereas the experimental results were obtained through laboratory testing experiments. It is noted the

obtained of a good agreement between the two curves with the convergence of the results. All this confirms both the accuracy and the mathematical credibility of the adopted model [15].

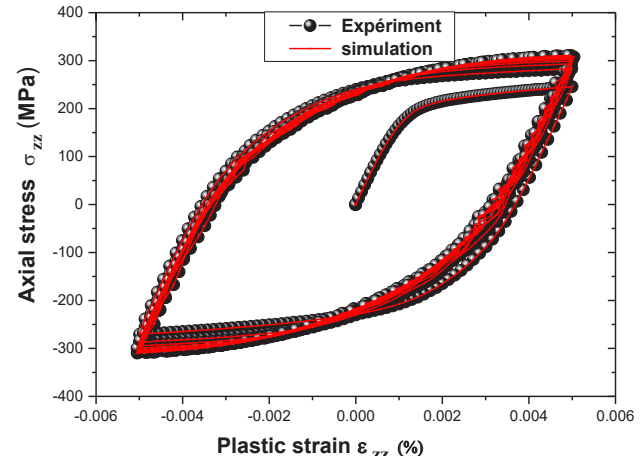


Fig. 2. Superposition of the experimental stabilized loop and simulation of 304L (SS)

3.2. Simulation on 304L (SS) using Prager Law

Using Prager law model, the numerical computation is done on 304L stainless steel for imposed value of strains of 0.5% and 1%, respectively, in order to analyze the material behavior.

3.2.1. Isotropic hardening simulation

The results of the numerical simulations are reported in Fig. 3.

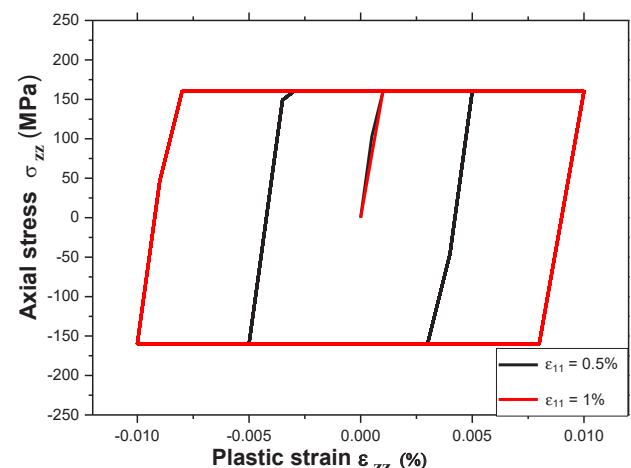


Fig. 3. Isotropic hardening according to Prager law

This figure shows the obtained hysteresis loops with isotropic hardening, from simulations on 304L stainless steel using Prager law, for two imposed strain of 0.5% and 1%. It can be noted that indicates that the hysteresis loop corresponding to 0.5% strain is narrower than the one obtained for 1% strain, which reveals an increase in stress accompanying with superior plastic energy dissipation.

From Fig. 3, it is showed the existence of symmetry in tension and compression. This reveals isotropic hardening; moreover, the non-appearance of translation of the loop centers shows that Prager model law does not account for kinematic hardening.

3.2.2. Linear kinematic hardening simulation

Fig. 4 is a reproduction of results in form of hysteresis loops for 304L stainless steel under application of two imposed strain levels, 0.5% and 1%, using a linear kinematic hardening model. The curve loops exhibit a progressive translation of their center during the cycles, which is characteristic of kinematic hardening behavior.

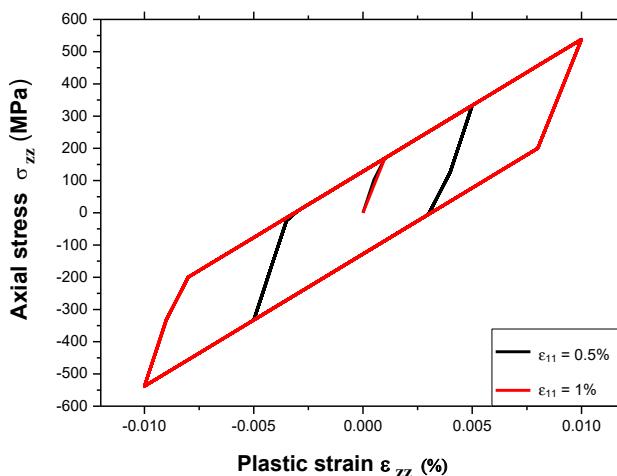


Fig. 4. Linear kinematic hardening

The linearity of the kinematic model doesn't permit a good representing certain nonlinear macroscopic phenomenon that can be observed in real situation.

3.3. Simulation on 304L (SS) using Chaboche law

3.3.1. Nonlinear kinematic hardening simulation

Fig. 5 illustrates the hysteresis loops simulated for 304L stainless steel under two imposed strain levels by employment of a nonlinear kinematic hardening model.

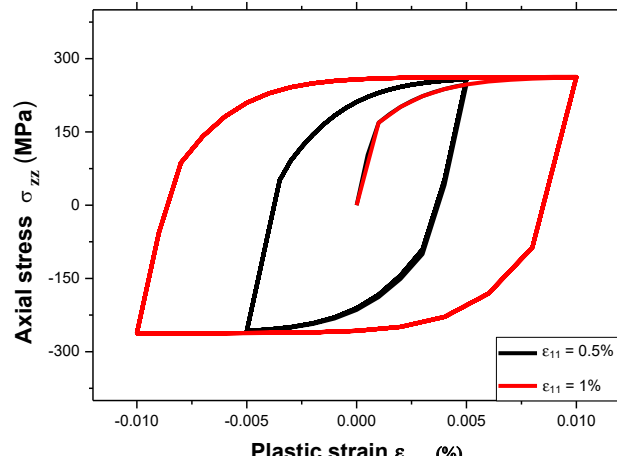


Fig. 5. Nonlinear kinematic hardening

The hysteresis loops are well curved representing the nonlinearity present in material. It can provide a more accurate description of the plastic behavior.

3.3.2. Combined hardening (Isotropy + Nonlinear kinematic)

Fig. 6 illustrates the behavior resulting from the combined effect of isotropic and kinematic hardening. The formation of hysteresis loops can be observed for two strain levels: 0.5% and 1%. The evolution of the size of the yield surface indicated the increase of the yield strength as a function of accumulated plastic strain. All this reflect isotropic hardening. In other hand, the translation of yield surface in the stress space demonstrates the occurrence of kinematic hardening.

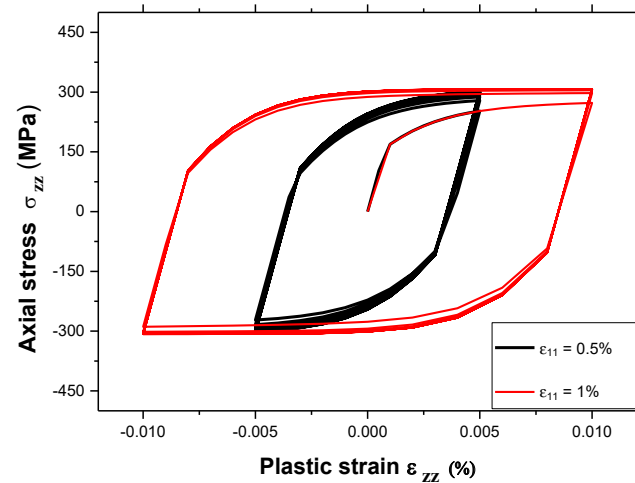


Fig. 6. Isotropic hardening and nonlinear kinematic hardening

Figs. 7, 8 show results of the application of two levels of imposed strain with value (0.5%) and (1%).

The superposition of the curves, have the objective of comparing the two used models. Prager model represents a simple linear kinematic hardening, but Chaboche model add the nonlinear kinematic hardening.

This comparison allows, evaluating the influence of nonlinear effects on cyclic behavior, particularly through the coupling of isotropic and nonlinear kinematic hardening, as illustrated by the shape of the curves.

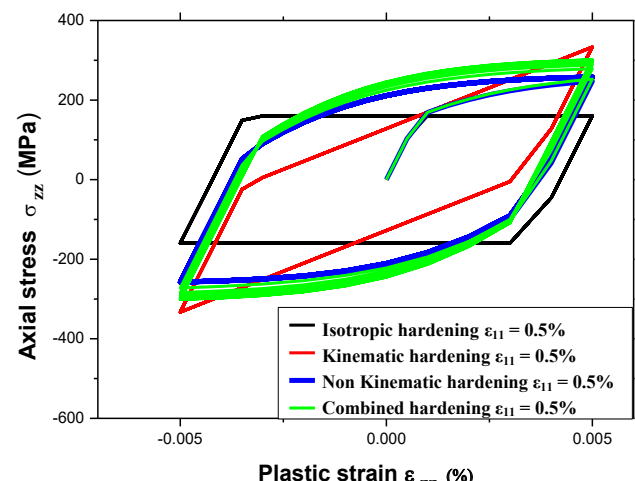


Fig. 7. Superposition between different hardenings for 304L steel with imposed strain (0.5%)

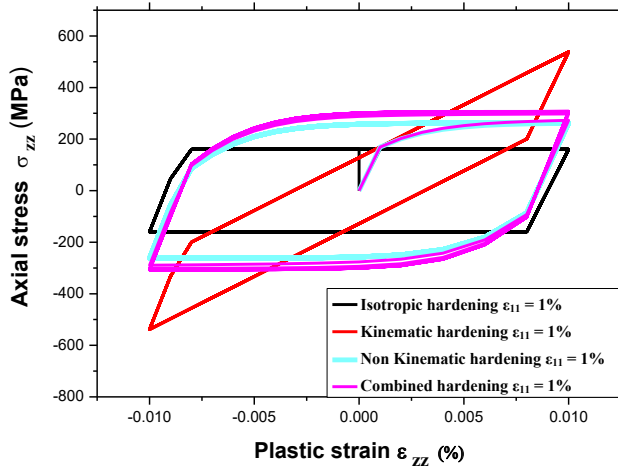


Fig. 8. Superposition of the different hardenings for 304L steel with imposed strain (1%)

3.4. Uniaxial strain-controlled

3.4.1. Loading histories

Numerical computations were performed on the 304L material by using Chaboche model law in order to study and analyze its behavior for its structural and industrial implementation. These were carried out by applying imposed strain rates, following loading histories H1 and H2, respectively, in the uniaxial direction (Table 3).

Figs. 9, 10 illustrate hysteresis curves of the results of corresponding two applied strain levels, 0.5% and 1%, revealing the re-

lationship between axial stress and plastic strain under application of cyclic loading.

From all the results, it can be observed that the wider loop represents the most greater strain amplitude in the specimen. It can be seen a greater energy dissipation and a more pronounced plastic behavior. The phenomenon of hardening is present due to the increase in stress during plastic strain.

3.4.2. Superposition of two curves

Fig. 11 illustrates the hysteresis loops obtained for two imposed strain levels: 0.5% (in black) and 1% (in blue). It can be observed that increasing the strain amplitude leads to a significant widening of the loops, indicating greater energy dissipation and an enhanced plastic behavior. The phenomenon of hardening is present due to the increase in stress during plastic strain.

These results confirm the ability of the Chaboche model to reproduce the effects of cyclic loading at different strain amplitudes.

3.5. Multiaxial strain-controlled loading

This investigation illustrates the evaluation of the behavior of 304L steel under application of biaxial cyclic cross-loading using two loading histories:

- the first history involves strain-controlled tension-compression cycles of $\pm 0.5\%$ for 10 cycles, followed by an equivalent torsional strain of $\pm 0.86\%$;
- in the second history, an axial strain of $\pm 1\%$ is applied, followed by an equivalent torsional strain of $\pm 1.73\%$, also for 10 cycles (Table 4).

Table 3

Loading conditions

Loading path	Loading history	Reference	Tensile/compression		Torsion	
			ε _{max} , %	ε _{min} , %	γ _{max} , %	γ _{min} , %
	H1	Fig. 9	+0.5	-0.5	0	0
	H2	Fig. 10	+1	-1	0	0

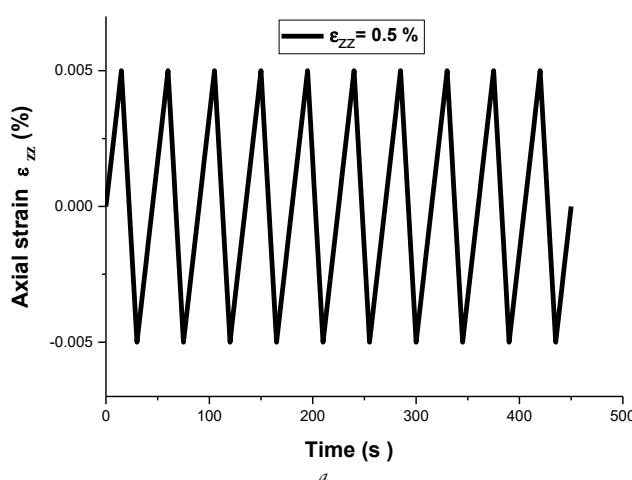
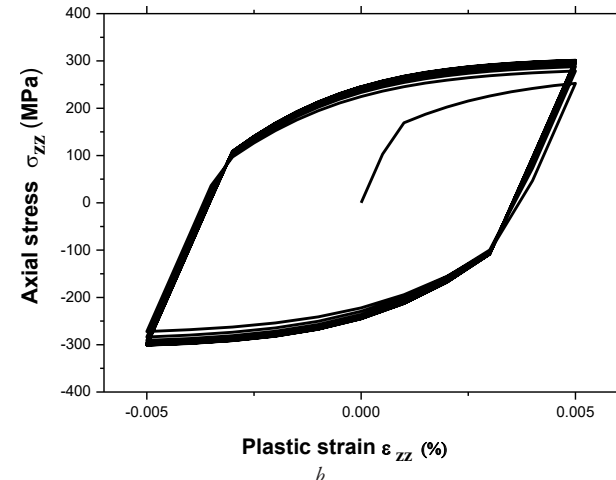


Fig. 9. Behavior of 304L SS under uniaxial loading for 0.5%: a – imposed strain as a function of time; b – hysteresis loops



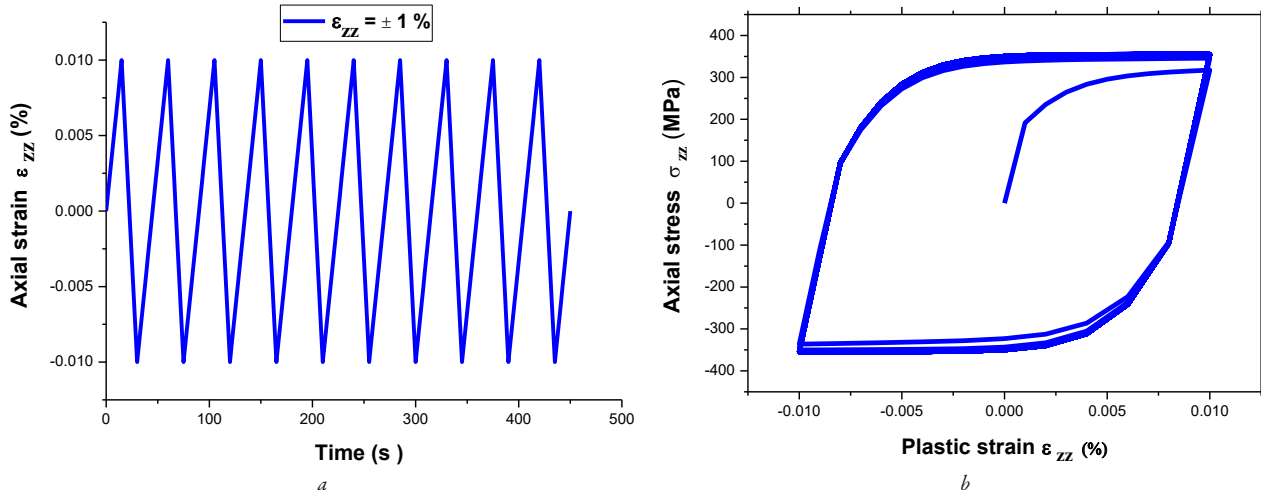


Fig. 10. Behavior of 304L SS under uniaxial loading for 1%, imposed strain as: *a* – function of time (H2); *b* – hysteresis loops

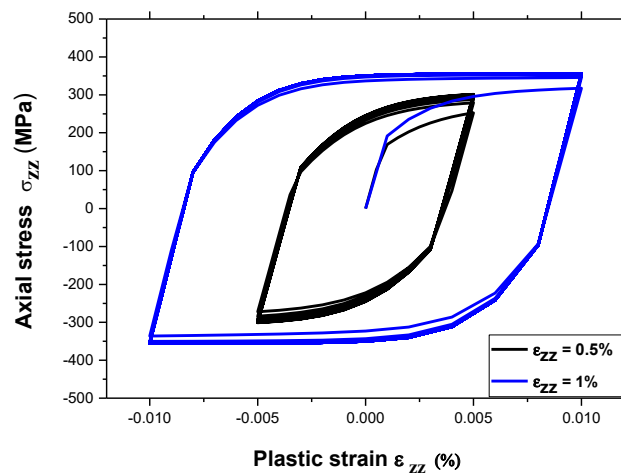


Fig. 11. Behavior of 304L SS under uniaxial loading for 0.5% and 1%

Table 4

Loading conditions in biaxial loading

Loading path	Loading history	Reference	Tensile/compression		Torsion	
			ϵ_{max} , %	ϵ_{min} , %	γ_{max} , %	γ_{min} , %
	H3	Fig. 12	+0.5	-0.5	+0.865 0.0086	-0.865 0.0086
	H4	Fig. 13	+1	-1	+1.73	-1.73

Fig. 12, *a* and Fig. 13, *a* show the evolution of axial strain and equivalent shear strain over time under multiaxial cyclic loading.

Both signals appear to be almost in phase, which suggests a proportional loading path. Fig. 12, *b* and Fig. 13, *b* are presentation of hysteresis loops associated with cyclic plastic behavior on material. It is found that the maximum stress that occur reaches approximately +300 MPa. The phenomenon of over-hardening is already clearly evident, in the case of cross-loading applied, as indicated by the increase in stress, in

the second loading direction, with a progressive strengthening, of the material during successive cycles.

3.6. Cyclic stress-controlled simulation

3.6.1. Ratcheting uniaxial 1D

The tensile-compression simple test is done by imposing two extreme asymmetrical stresses at 50 cycles on material with progressive stress amplitude and constant average stress (Table 5).

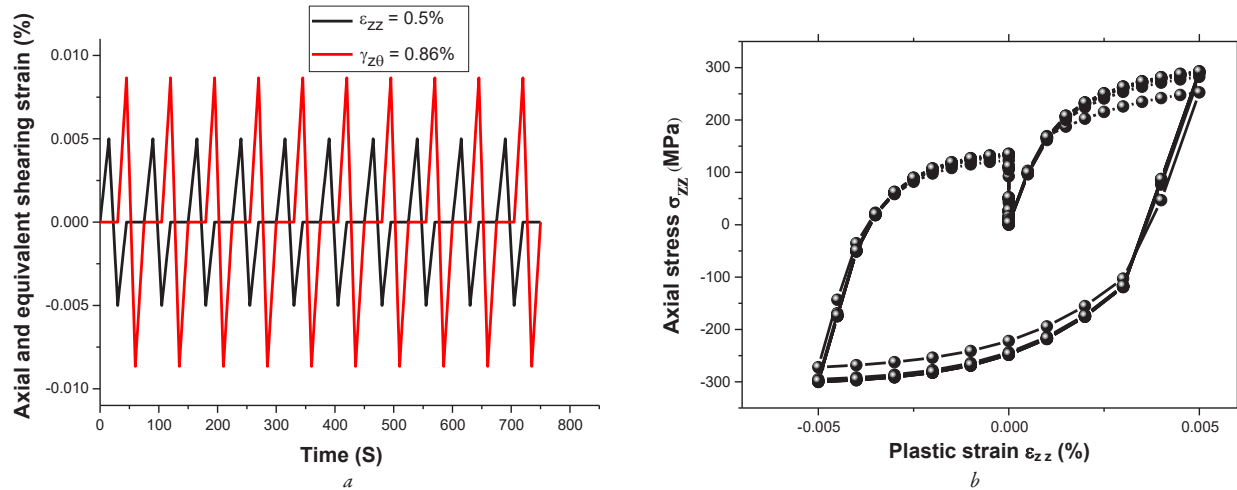


Fig. 12. Behavior of 304L SS for 0.5% under biaxial loading: *a* – axial and angular strain as a function of time; *b* – evolution of stress versus plastic strain

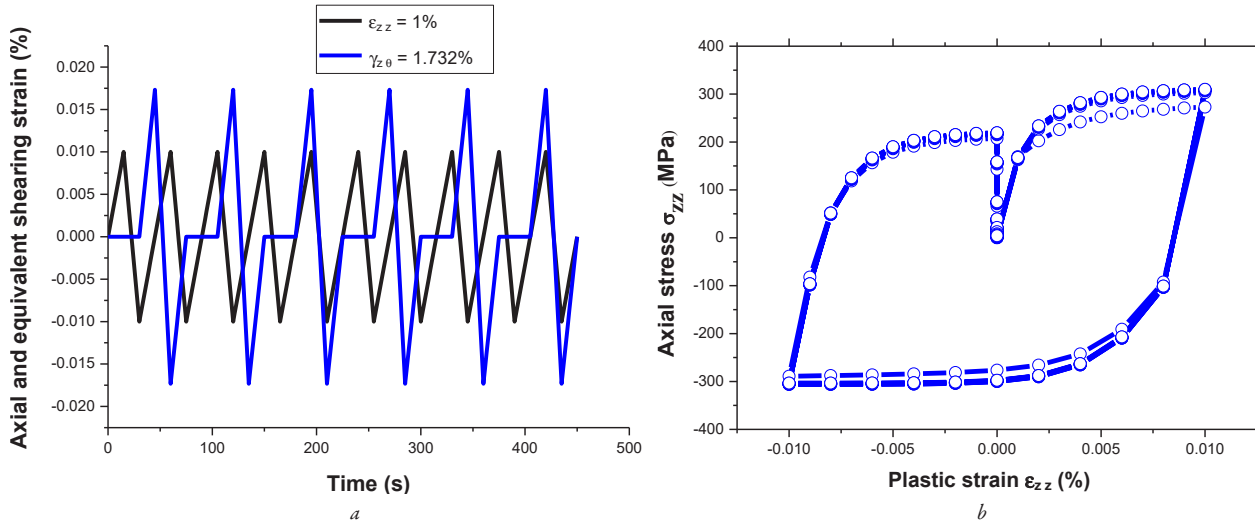


Fig. 13. Behavior of 304L SS for 1% under biaxial loading: *a* – axial and angular strain as a function of time; *b* – evolution of stress versus plastic strain

Table 5
Stories, loading path, imposed stresses

Stories, loading path, imposed stresses		
	$\sqrt{3}\sigma_{z0}$ Mean	
	σ_x	
		Loading, MPa
Axial stress	σ_{\max}	275
	σ_{\min}	-75
Mean stress	$\sigma_{\text{mean}} = \frac{\sigma_{\max} + \sigma_{\min}}{2}$	100
Stress amplitude	$\sigma_a = \frac{\sigma_{\max} - \sigma_{\min}}{2}$	175
Shear stress	$\sqrt{3}\sigma_{z0} \text{ max}$	0
	$\sqrt{3}\sigma_{z0} \text{ min}$	0

Table 5

2. The stress amplitude remains constant: the maximum and minimum stresses are nearly stable, confirming that the test was performed under stress-controlled conditions.

3. The stresses reach up to 275 MPa, suggesting that the behavior falls within the low-cycle fatigue domain, where ratcheting becomes particularly critical.

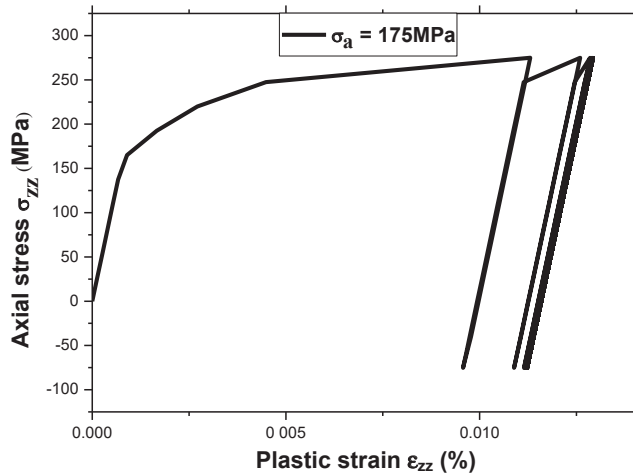


Fig. 14. Uniaxial 1D ratcheting of 304L steel for ($\sigma_{\text{mean}} = 100$ MPa, $\sigma_a = 175$ MPa)

Fig. 14 shows a cyclic relationship between axial stress and axial strain under tension-compression loading with a non-zero mean stress.

The following observations can be made:

1. The hysteresis loops progressively shift to the right, indicating an accumulation of plastic strain, which is characteristic of the ratcheting phenomenon.

3.6.2. Ratcheting biaxial 2D

A cross stress-controlled test was performed, consisting of one tension-compression cycle ranging from 200 MPa to -150 MPa, followed by one shear cycle with stress varying between 150 MPa and 100 MPa (Table 6).

Stories, loading path, imposed stresses

		Loading, MPa
Axial stress	σ_{\max}	+200
	σ_{\min}	-150
Mean stress	$\sigma_{\text{mean}} = \frac{\sigma_{\max} + \sigma_{\min}}{2}$	+25
Stress amplitude	$\sigma_a = \frac{\sigma_{\max} - \sigma_{\min}}{2}$	+175
Shear stress	$\sqrt{3}\sigma_{\text{sg}} \text{ max}$	+150
	$\sqrt{3}\sigma_{\text{sg}} \text{ min}$	-100

The obtained results of loop cycles under biaxial cyclic loading applied at constant stress are presented of Fig. 15. It can have deduced the following observations from all results:

- application of cyclic loading produces a non-zero average stress, making an anomaly caused the appearance of phenomena noted the ratchet effect;
- change of cycles progressively towards increasing plastic strain values, demonstrating an accumulation progressive of deformation;
- it detects a high stress levels, reaching approximately the value of ± 200 MPa. This corresponds to the low-cycle fatigue range, within which the ratchet phenomena effect can occur.

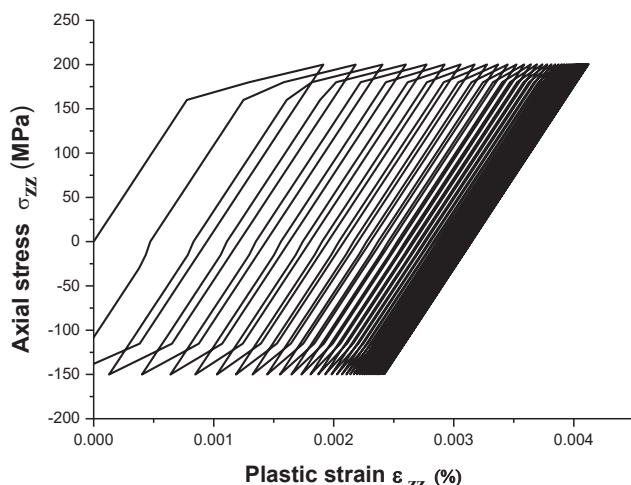


Fig. 15. Ratcheting biaxial 2D of 304L steel for ($\sigma_{\text{mean}} = 25$ MPa, $\sigma_a = 175$ MPa)

Ratcheting under uniaxial and biaxial cyclic loading is one of the most critical phenomena affecting the integrity of engineering structures. This effect represents a major risk in many industrial applications, as it can lead to progressive deformation and ultimately severe structural damage or failure. In such cases, the likelihood of spontaneous failure remains high regardless of the applied mean stress value.

In the present research, the most relevant and widely used constitutive models for accurately describing the in-service behavior of

engineering materials are identified and examined. To realistically predict material response and contribute to the prevention of structural failure, materials must be subjected to various cyclic loading scenarios by specialists. Among the available plasticity models, the linear Prager model and the nonlinear Chaboche model remain the most frequently applied in the fatigue analysis of materials and structures. The Chaboche model, established and expanded across several foundational works [1, 2, 14], has been widely adopted for its ability to reproduce complex cyclic phenomena.

Numerous researchers have investigated the effectiveness of the Chaboche model in describing ratcheting and cyclic plasticity across different materials and temperature ranges. Recent studies confirm its capability to capture nonlinear kinematic hardening, ratcheting accumulation, and hysteresis loop evolution under uniaxial and multiaxial loading [3–5]. Experimental and numerical analyses on stainless steels also highlight the superior accuracy of the Chaboche model when compared with simpler linear hardening laws, particularly for predicting multiscale and stress-path-dependent deformation mechanisms [6, 9, 10].

Comparisons between the Prager and Chaboche models consistently show the limitations of the linear Prager formulation in reproducing ratcheting, mean stress relaxation, or cyclic stabilization. In contrast, the nonlinear multi-component Chaboche model effectively replicates macroscopic phenomena such as strain growth, cyclic hardening/softening, and hysteresis loop translation, as demonstrated in several investigations on stainless steels and aluminum alloys [7, 8, 11–13]. Accurate prediction of cyclic behavior also depends strongly on the identification of material parameters, as demonstrated in parameter-sensitivity studies [15].

Extensive numerical results obtained using the Chaboche model under uniaxial and multiaxial loading covering diverse stress and strain amplitudes confirm its suitability for improving fatigue life predictions and supporting the design of structures exposed to service cyclic loading. The analysis of one-dimensional and two-dimensional ratcheting phenomena through hysteresis loop evolution further strengthens its applicability to industrial cases.

3.7. Limitations and future directions of the research

When using Prager or Chaboche models to describe the behavior of 304L stainless steel, several limitations must be considered. Both models rely on simplifying assumptions, such as material homogeneity and isotropy, and often neglect temperature, microstructural effects, and strain-rate sensitivity. Prager linear kinematic hardening cannot capture cyclic phenomena such as ratcheting, mean stress relaxation, or complex softening/hardening, while even the more advanced Chaboche model may be limited under multiaxial, non-proportional, or extreme loading conditions.

For future work, the research could be extended to more complex geometries to generalize the current findings. Considering additional factors such as temperature fluctuations, environmental conditions, and long-term aging would further enhance the practicality and accuracy of the adopted constitutive models.

4. Conclusions

1. In this research, a demonstration with the use a perfect numerical simulation, these tools are an efficient method to analysis and predicts the material behavior and performance of 304L stainless steel used to make components, consequently allowing more safe and optimal designs in structural applications. The superposition of the numerical and experimental results of cyclic loading on 304L is in good agreement. The superposition of the numerical and experimental results of cyclic loading on 304L is in good agreement; it is presented results by the hysteresis curves obtained under an imposed plastic strain of 0.5%.
2. The simple linear model noted by Prager model offers a good description of kinematic hardening but in other hand cannot show the

nonlinear effects such as over-hardening or ratcheting. In difference, the more complex model noted by Chaboche model can when used accurately reproduces the uniaxial hardening, controls over-hardening, and ratcheting behavior. It is noted the presence symmetry in tension and compression noted the isotropic hardening.

3. The results obtained from this research gives a comparative analysis to be able to evaluate with the two models, the effects of taken in consideration isotropic and nonlinear kinematic hardening on cyclic material behavior in 304L stainless steel. It is known that simple isotropic hardening effectively can describes the monotonic hardening but it is not used to represent the effects of cyclic loading and mean stress evolution. From this, combined isotropic-kinematic hardening models can significantly be used to improve the predictions and the capturing of the initial hardening and the subsequent stabilization of hysteresis loops. The obtained results from the use of the two models were presented with the growth and translation of surface in the stress space demonstrates the occurrence of kinematic hardening.

4. In conclusion, when using the Chaboche model it is possible to say that this model is the most suitable and reliable constitutive formulation for the simulation of material behavior when exposed to the cyclic elastoplastic behavior of 304L stainless steel and for supporting fatigue life prediction and structural design under complex loading conditions. From that, it is a confirmation of the ability of the Chaboche model to reproduce the effects of cyclic loading at different strain amplitudes.

Conflict of interest

The authors declare that they have no conflict of interest in relation to this research, including financial, personal, authorship or other, which could affect the research and its results presented in this article.

Financing

The research was performed without financial support.

Data availability

The manuscript has no linked data.

Use of artificial intelligence

The authors confirm that they did use artificial intelligence technologies ChatGPT-4.0 was used to search for literature, and to check grammar, spelling, and punctuation.

The authors bear full responsibility for the final manuscript. Declaration submitted by Kamel Fedaoui.

Authors' contributions

Amira Aboussalih: Conceptualization, Methodology, Writing – original draft; **Salah Hammoudi:** Writing – review and editing; **Kamel Fedaoui:** Methodology, Investigation, Visualization, Writing – review and editing; **Karim Arar:** Formal analysis, Writing – original draft; **Lazhar Baroura:** Methodology, Investigation, Formal analysis, Visualization, Writing – original draft.

References

1. Chaboche, J.-L. (1981). Continuous damage mechanics – A tool to describe phenomena before crack initiation. *Nuclear Engineering and Design*, 64 (2), 233–247. [https://doi.org/10.1016/0029-5493\(81\)90007-8](https://doi.org/10.1016/0029-5493(81)90007-8)
2. Chaboche, J. L. (2008). A review of some plasticity and viscoplasticity constitutive theories. *International Journal of Plasticity*, 24 (10), 1642–1693. <https://doi.org/10.1016/j.ijplas.2008.03.009>
3. Subasic, M., Alfredsson, B., Dahlberg, C. F. O., Öberg, M., Efsing, P. (2023). Mechanical Characterization of Fatigue and Cyclic Plasticity of 304L Stainless Steel at Elevated Temperature. *Experimental Mechanics*, 63 (8), 1391–1407. <https://doi.org/10.1007/s11340-023-00992-5>
4. Azizoğlu, Y., Lindgren, L.-E. (2024). Temperature and plastic strain dependent Chaboche model for 316 L used in simulation of cold pilgering. *International Journal of Material Forming*, 18 (1). <https://doi.org/10.1007/s12289-024-01864-6>
5. Skrzat, A., Wójcik, M. (2023). Explicit and Implicit Integration of Constitutive Equations of Chaboche Isotropic-Kinematic Hardening Material Model. *Acta Metallurgica Slovaca*, 29 (4), 200–205. <https://doi.org/10.36547/ams.29.4.1949>
6. Belattar, A., Taleb, L. (2021). Experimental and numerical analyses of the cyclic behavior of austenitic stainless steels after prior inelastic histories. *International Journal of Pressure Vessels and Piping*, 189, 104256. <https://doi.org/10.1016/j.ijpvp.2020.104256>
7. Kebir, T., Benguadiab, M., Miloudi, A., Imad, A. (2017). Simulation of The Cyclic Hardening Behavior of luminum Alloys. *Scientific Bulletin-University Politehnica of Bucharest. Series D*, 79 (4), 240–250. Available at: https://www.scientificbulletin.upb.ro/rev_docs_arhiva/rezb11_236576.pdf
8. Boussalih, F., Meziani, S., Fouathia, A., Fedaoui, K. (2019). Behavior of 304L stainless steel under uniaxial loading and effect of the mean stress on the ratcheting by simulation using Chaboche model. *Scientific Bulletin-University Politehnica of Bucharest. Series D*, 81 (2), 179–190. https://www.scientificbulletin.upb.ro/rev_docs_arhiva/fullae_340862.pdf
9. Acar, S. S., Yalçinkaya, T. (2025). Modeling of the Stress Path-Dependent Strain Ratcheting Behaviour of 304L Stainless Steel Through Crystal Plasticity Frameworks. *Metals and Materials International*, 31 (9), 2525–2540. <https://doi.org/10.1007/s12540-025-01907-w>
10. Taleb, L., Hauet, A. (2009). Multiscale experimental investigations about the cyclic behavior of the 304L SS. *International Journal of Plasticity*, 25 (7), 1359–1385. <https://doi.org/10.1016/j.ijplas.2008.09.004>
11. Delobel, P., Robinet, P., Bocher, L. (1995). Experimental study and phenomenological modelization of ratchet under uniaxial and biaxial loading on an austenitic stainless steel. *International Journal of Plasticity*, 11 (4), 295–330. [https://doi.org/10.1016/s0749-6419\(95\)00001-1](https://doi.org/10.1016/s0749-6419(95)00001-1)
12. Boussalih, F., Fedaoui, K., Zarza, T. (2022). Chaboche Model for Fatigue by Ratcheting Phenomena of Austenitic Stainless Steel under Biaxial Sinusoidal Loading. *Civil Engineering Journal*, 8 (3), 505–518. <https://doi.org/10.28991/cej-2022-08-03-07>
13. Mazánová, V., Polák, J., Škorík, V., Kruml, T. (2017). Multiaxial elastoplastic cyclic loading of austenitic 316L steel. *Frattura Ed Integrità Strutturale*, 11 (40), 162–169. <https://doi.org/10.3221/igf-esis.40.14>
14. Chaboche, J. L. (1989). Constitutive equations for cyclic plasticity and cyclic viscoplasticity. *International Journal of Plasticity*, 5 (3), 247–302. [https://doi.org/10.1016/0749-6419\(89\)90015-6](https://doi.org/10.1016/0749-6419(89)90015-6)
15. Djimli, L., Taleb, L., Meziani, S. (2010). The role of the experimental data base used to identify material parameters in predicting the cyclic plastic response of an austenitic steel. *International Journal of Pressure Vessels and Piping*, 87 (4), 177–186. <https://doi.org/10.1016/j.ijpvp.2010.02.002>

Amira Aboussalih, Researcher, Department of Mechanic, Institute of Applied Sciences and Techniques (ISTA), University Frères Mentouri Constantine 1, Constantine, Algeria, ORCID: <https://orcid.org/0009-0000-5783-5429>

Salah Hammoudi, Researcher, Department of Mechanic, Institute of Applied Sciences and Techniques (ISTA), University Frères Mentouri Constantine 1, Constantine, Algeria, ORCID: <https://orcid.org/0009-0008-0382-1206>

✉ **Kamel Fedaoui**, PhD, The Laboratory of Renewable Energy, Energy Efficiency and Smart Systems (LEREESI), Higher National School of Renewable Energy, Environment & Sustainable Development (RE2SD), Batna, Algeria, ORCID: <https://orcid.org/0000-0003-0885-6914>, e-mail: K.fedaoui@hns-re2sd.dz

Lazhar Baroura, Researcher, Department of Mechanic, Institute of Applied Sciences and Techniques (ISTA), University Frères Mentouri Constantine 1, Constantine, Algeria, ORCID: <https://orcid.org/0000-0002-6747-5049>

Karim Arar, Researcher, Department of Mechanic, Batna 2 University, Batna, Algeria, ORCID: <https://orcid.org/0009-0004-5951-0846>

✉ Corresponding author